24th COBEM - 2017

24th ABCM International Congress of Mechanical Engineering
December 3-8, 2017, Curitiba, PR, Brazil

# COBEM-2017-2568
# ESTIMATION OF THE THERMAL CONDUCTANCE AT THE CONTACT INTERFACE OF A LAMINATED COMPOSITE WITH THE UNSCENTED KALMAN FILTER

**L. B. Florindo**
Federal University of Espírito Santo, Graduate Program in Mechanical Engineering, ES, Brazil
leonebf@hotmail.com

**L. A. S. Abreu**
**D. C. Knupp**
Rio de Janeiro State University, Department of Mechanical Engineering, RJ, Brazil
abreu.l@gmail.com; diegoknupp@iprj.uerj.br

**J. C. S. Dutra**
**W. B. Silva**
Federal University of Espírito Santo, Graduate Program in Chemical Engineering Program, ES, Brazil
julio.dutra@ufes.br; wellingtonufes@gmail.com

***Abstract.*** *The adhesion failures between the layers of a composite material are related to the thermal contact conductance, therefore this work aims to estimate this parameter in a laminated composite. To solve the direct problem, the Method of Lines was applied, while the inverse problem was solved by a Bayesian filter called Unscented Kalman Filter. The physical problem used in this study is composed of a plate with two layers, so the heat transfer problem has two spatial dimensions and a time dimension. Then, the values assigned for thermal conductance on interface layer depends on time and space. In this work, in order to analyze the proposed methodology, simulated temperature measurements were used. The results reveal the capability of the proposed approach.*

***Keywords:*** *Inverse problems, Bayesian filters, Thermal contact conductance, Unscented Kalman Filter.*

## 1. INTRODUCTION

Composites are made combining two or more materials, usually with properties much different aiming to achieve a new material with special features, therewith, its use has been applied in the aerospace and automotive industry, civil structure, among others (Gay *et al*., 2003; Rezende and Botelho, 2000).

The structure of a composite contains two phases, a matrix which is a continuous phase and the reinforcement also known as dispersed phase. The classification can be defined according to the constituent materials. However, the dispersion phase is generally classified as: particulate, fiber reinforced and structural laminate (Ventura, 2009).

Rezende and Botelho (2000) reported numerous advantages related to the use of composites, such as: carbon/carbon composites have high corrosion resistance and good thermal and electrical properties; polymer composites reinforced with carbon fiber have good radiofrequency reflection properties; high dimensional stability and good electrical conductivity, and the composites with glass fibers have features of being transparent to the electromagnetic radiation in the microwave range.

The composite materials also have some disadvantages. Lee and Knauss (2000) have studied the failures due discontinuous thickness under high loads and high temperatures in laminated composites.

In the literature, some recent researches to detect composite failures can be found. Abreu *et al*. (2014) solved an inverse problem to estimate the contact failures in multi-layered composites. In their work, the direct problem was solved through a hybrid method formed joining the generalized integral transformation technique with finite differences. In the inverse problem, Bayesian inference was used with a Markov Chain Monte Carlo method. The results indicated that the failures were perfectly identified and it was also stated that the technique used was robust in relation to measurement errors.

Burghold *et al*. (2015) studied the thermal contact conductance as a function of time through an assay which a high-speed infrared camera was used to measure the temperatures of the tested material, these measurements being used to determine the thermal conductance at the interface. The samples were heated up separately with different heat fluxes until reaching a steady-state temperature. Then, they were placed in contact and submitted to different loads in order to observe the behavior of contact heat transfer coefficient. The results showed that the heat transfer is related to the intensity of the applied load, this fact may be caused by the elastic resilience which sustains the contact area.

In this paper, the direct problem is solved within the Method of Lines (MOL), while the inverse problem is solved by a Bayesian filter called Unscented Kalman Filter (UKF). The physical problem used in this study is composed of two spatial dimensions and a time dimension, so that the values assigned for thermal conductance depends on time and space. The temperature measurements for the experiment were acquired through simulations, where the direct problem model was used and noises were added to represent a real measurement case, which invariably has uncertainties due equipment limitations. Different magnitudes of noise were applied to afford robust results.

## 2. PHYSICAL PROBLEM

The physical problem consists of two plates with different properties, which have one of the edges in common forming a contact interface, where it is desired to find the thermal conductance $h_c(t,x)$. A constant heat flux $q(t,x)$ is applied to one of the edges of the plate *2* as can be seen from Fig. 1.

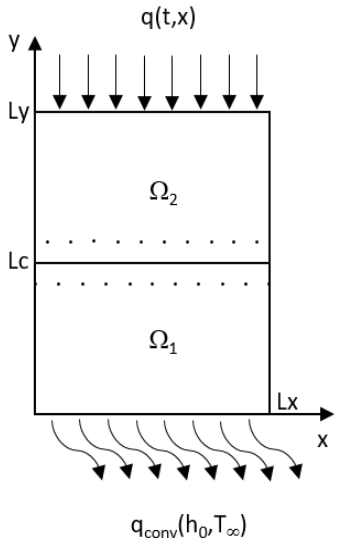


Figure 1. Physical problem - heat transfer

The lengths of the plate *1* and *2* are represented by *Lc* and *Ly-Lc*, respectively, whereas the width is denoted by *Lx*. The convective heat flux $q_{conv}(h_0,T_\infty)$ is a function of heat transfer coefficient $h_0$ and environment temperature $T_\infty$. The equations that represent the problem are showed from Eq. (1) to (10):

$$\frac{1}{\alpha_1}\frac{\partial T_1}{\partial t} = \frac{\partial^2 T_1}{\partial x^2} + \frac{\partial^2 T_1}{\partial y^2} \quad at \quad \begin{matrix} 0 < x < Lx \\ 0 < y < Lc \end{matrix} ; \quad t > 0 \tag{1}$$

$$\frac{1}{\alpha_2}\frac{\partial T_2}{\partial t} = \frac{\partial^2 T_2}{\partial x^2} + \frac{\partial^2 T_2}{\partial y^2} \quad at \quad \begin{matrix} 0 < x < Lx \\ Lc < y < Ly \end{matrix} ; \quad t > 0 \tag{2}$$

$$-k_1\frac{\partial T_1}{\partial y} + h_0 T_1 = h_0 T_\infty \quad at \quad \begin{matrix} 0 < x < Lx \\ y = 0 \end{matrix} ; \quad t > 0 \tag{3}$$

$$k_2\frac{\partial T_2}{\partial y} = q(t,x) \quad at \quad \begin{matrix} 0 < x < Lx \\ y = Ly \end{matrix} ; \quad t > 0 \tag{4}$$

$$\left.\begin{array}{c} k_1 \dfrac{\partial T_1}{\partial y} = k_2 \dfrac{\partial T_2}{\partial y} \\ k_1 \dfrac{\partial T_1}{\partial y} = h_c(t,x)(T_2 - T_1) \end{array}\right\} \quad at \quad \begin{array}{c} 0 < x < Lx \\ y = Lc \end{array} \quad ; \quad t > 0 \tag{5}$$

$$\frac{\partial T_1}{\partial x} = 0 \quad at \quad \begin{array}{c} x = 0 \\ 0 < y < Lc \end{array} \quad ; \quad t > 0 \tag{6}$$

$$\frac{\partial T_1}{\partial x} = 0 \quad at \quad \begin{array}{c} x = Lx \\ 0 < y < Lc \end{array} \quad ; \quad t > 0 \tag{7}$$

$$\frac{\partial T_2}{\partial x} = 0 \quad at \quad \begin{array}{c} x = 0 \\ Lc < y < Ly \end{array} \quad ; \quad t > 0 \tag{8}$$

$$\frac{\partial T_2}{\partial x} = 0 \quad at \quad \begin{array}{c} x = Lx \\ Lc < y < Ly \end{array} \quad ; \quad t > 0 \tag{9}$$

$$T_1 = T_2 = T_\infty \quad \forall \quad \Omega_1 \cup \Omega_2 \; ; \quad t = 0 \tag{10}$$

where $\Omega$ is a domain with thermal diffusivity $\alpha$, thermal conductivity $k$, and temperature $T$. The subscripts numbers *1* and *2* refer to each plate.

In the estimation of the $h_c(t,x)$, it is considered that the measured temperatures can be obtained at every spots of the plates by an infrared thermal camera, but aiming to verify the results with a reduced number of measured temperatures, the thermal contact conductance will still be estimated using only 21 temperature measurements distributed according to the points represented in Fig. 1. In this experiment, the measured temperatures were obtained through simulations.

The algorithms were written in MATLAB software and run on a computer with configuration as Intel Core i5 and 8GB of Random Access Memory.

### 2.1 Direct Problem Solution

For the solution of the direct problem, the Method of Lines was used, which is considered a special finite difference method that achieves a good accuracy with a significantly lower computational effort when compared with the common finite difference method. The method can be summarized in discretizing some variables of the partial differential equation (PDE) reducing to an ordinary differential equation (ODE) that may be solved analytically (Sadiku and Obiozor, 2000).

In Fig. 2, the domain discretized on grid is schematically presented, where the index *i* and *j* are defined as *i = 1, 2, ..., ny* and *j = 1, 2, ..., nx*, respectively, the number of nodes at *x* direction is denoted by *nx* and at *y* direction by *ny*.

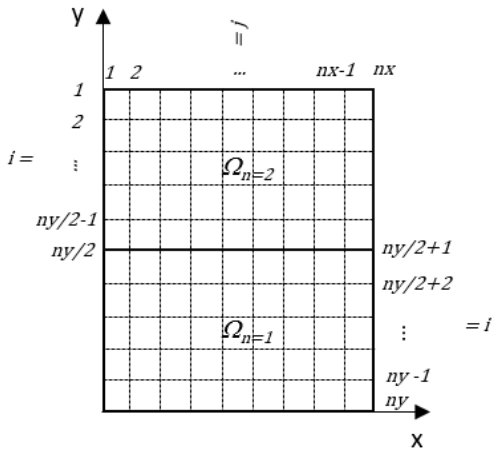


Figure 2. Finite difference

Applying central difference at second-order derivatives of Eq. (1) and (2), an approximation is obtained as can be seen in Eq. (11), that it is a generic equation, where *n* can adopt the value *1* or *2* representing each plate, $\Delta x = Lx/(nx-1)$ and $\Delta y = Ly/(ny-1)$.

$$\frac{\partial T_{n(i,j)}}{\partial t} = \alpha_n \left( \frac{T_{n(i+1,j)} - 2T_{n(i,j)} + T_{n(i-1,j)}}{\Delta y^2} + \frac{T_{n(i,j+1)} - 2T_{n(i,j)} + T_{n(i,j-1)}}{\Delta x^2} \right) \tag{11}$$

For the first-order derivatives was applied a forward/backward difference approximation with third order error with respect to the variable *y*, as shown Eq. (12) and (13).

$$\frac{\partial T_n}{\partial y} = \frac{-T_{n(i+2,j)} + 6T_{n(i+1,j)} - 3T_{n(i,j)} + 2T_{n(i-1,j)}}{6\Delta y} \tag{12}$$

$$\frac{\partial T_n}{\partial y} = \frac{2T_{n(i+1,j)} + 3T_{n(i,j)} - 6T_{n(i-1,j)} + T_{n(i-2,j)}}{6\Delta y} \tag{13}$$

For the first-order derivatives with respect to the variable *x* was applied a forward/backward difference approximation with first order error written as following equations:

$$\frac{\partial T_n}{\partial x} = \frac{T_{n(i,j+1)} - T_{n(i,j)}}{\Delta x} \tag{14}$$

$$\frac{\partial T_n}{\partial x} = \frac{T_{n(i,j)} - T_{n(i,j-1)}}{\Delta x} \tag{15}$$

At this moment, the problem became in solving an ordinary differential equation with time-dependent vector which was solved by the *ode15s* function available in MATLAB software.

### 2.2 Inverse Problem Solution

For the estimation of thermal contact conductance (TCC), the UKF was applied, which it is an improvement of the Kalman filter that allows to be used in nonlinear systems (Wan and van der Merwe, 2000).

The idea of Unscented Kalman Filter method is to transform a Gaussian Random Variable (GRV) through a non-linear function and to approximate of a Gaussian distribution. It is used the Unscented Transformation (UT) method to allow this approximation (Julier and Uhlmann, 1997).

The UT use *2n+1* sigma points with their corresponding weights to approximate the mean $\bar{x}$ and covariance *P* by the following equations:

$$\begin{aligned} X_1 &= \bar{x} \\ X_i &= \bar{x} + A \qquad i = 2,3,\ldots,n+1 \\ X_i &= \bar{x} - A \qquad i = n+2,\ldots,2n+1 \end{aligned} \tag{16}$$

$$\begin{aligned} W_1^m &= \frac{\lambda}{n+\lambda} \\ W_i^m = W_i^c &= \frac{1}{2(n+\lambda)} \qquad i = 2,3,\ldots,2n+1 \\ W_1^c &= W_1^m + (1 - a^2 + b) \end{aligned} \tag{17}$$

where $A = ((n+\lambda)P)^{1/2}$, $\lambda = a^2(n + \kappa)-n$, *n* is the dimension of vector *x*, *a* and $\kappa$ are scaling parameter, *b* is use to consider prior knowledge about the distribution of *x*, *X* is the vector sigma, and *W* is the corresponding weights.

Each sigma point undergoes a non-linear function, then it is calculated the mean and covariance of new points as shown at from Eq. (18) to (20).

$$Y_i = f(X_i) \qquad i = 1,2,...,2n+1 \tag{18}$$

$$\bar{y} \approx \sum_{i=1}^{2n+1} W_i^m Y_i \tag{19}$$

$$P_y \approx \sum_{i=1}^{2n+1} W_i^c \left(Y_i - \bar{y}\right)\left(Y_i - \bar{y}\right)^T \tag{20}$$

The Bayesian filter (UKF) has direct application of the Unscented Transformation method and may be summarized according to the steps presented in the Box 1 and 2.

1. Calculate sigma points

$$B_k = [\underbrace{\bar{x}_k \quad ... \quad \bar{x}_k}_{n}]$$

$$X_k = [\bar{x}_k \quad B_k + A_k \quad B_k - A_k]$$

2. Transform each sigma point by the non-linear function

$$\hat{X}_{k+1} = f(X_k)$$

3. Calculate the predicted mean

$$\bar{x}_{k+1}^- = \sum_{i=1}^{2n+1} W_i^m \hat{X}_{i,k+1}$$

4. Calculate the predicted covariance

$$P_{k+1}^- = \sum_{i=1}^{2n+1} W_i^c \left(\hat{X}_{i,k+1} - \bar{x}_{k+1}^-\right)\left(\hat{X}_{i,k+1} - \bar{x}_{k+1}^-\right)^T + Q_k$$

5. Update sigma points

$$B_{k+1}^- = [\underbrace{\bar{x}_{k+1}^- \quad ... \quad \bar{x}_{k+1}^-}_{n}]$$

$$X_{k+1}^- = [\bar{x}_{k+1}^- \quad B_{k+1}^- + A_{k+1}^- \quad B_{k+1}^- - A_{k+1}^-]$$

6. Transform the prediction points by the observation model

$$Y_{k+1}^- = h(X_{k+1}^-)$$

7. Calculate the predicted observation

$$\hat{y}_{k+1}^- = \sum_{i=1}^{2n+1} W_i^m Y_{i,k+1}^-$$

8. Calculate the innovation covariance

$$P_{\tilde{y}_{k+1}\tilde{y}_{k+1}} = \sum_{i=1}^{2n+1} W_i^c \left(Y_{i,k+1}^- - \hat{y}_{k+1}^-\right)\left(Y_{i,k+1}^- - \hat{y}_{k+1}^-\right)^T + R_{k+1}$$

9. Calculate the cross-correlation matrix

$$P_{x_{k+1}y_{k+1}} = \sum_{i=1}^{2n+1} W_i^c \left(X_{i,k+1}^- - \bar{x}_{k+1}^-\right)\left(Y_{i,k+1}^- - \hat{y}_{k+1}^-\right)^T$$

Box 1. Unscented Kalman Filter Algorithm – Part 1

10. Calculate da Kalman gain

$$K_{k+1} = P_{x_{k+1}y_{k+1}} P^{-1}_{\tilde{y}_{k+1}\tilde{y}_{k+1}}$$

11. Calculate the posteriori state estimate

$$\bar{x}_{k+1} = \bar{x}^{-}_{k+1} + K_{k+1}(y_{k+1} - \hat{y}^{-}_{k+1})$$

12. Calculate the posteriori state covariance

$$P_{k+1} = P^{-}_{k+1} - K_{k+1} P_{\tilde{y}_{k+1}\tilde{y}_{k+1}} K^{T}_{k+1}$$

Box 2. Unscented Kalman Filter Algorithm – Part 2

## 3. RESULTS AND DISCUSSION

Some data inputs were extracted from Colaço and Alves (2015), Abreu *et al*. (2014) and Silva e*t al*. (2016). The analyzed materials were: AISI 1050 steel with $k$ = 54 W/(m°C) and $\alpha$ = 1.474x10$^{-5}$ m²/s, and Inconel with $k$ = 14 W/(m°C) and $\alpha$ = 3.428x10$^{-6}$ m$^2$/s. The dimension of each plate was 0.04m x 0.01m. The constant heat flux imposed was 10,000 W/m$^2$ during 50 minutes. The plates initially presented a temperature of 25 °C at all their extension and the convection heat transfer coefficient is equal to 0. For the simulation of temperature measurements, three different magnitudes of noise were added to represent the measurement error. The noises were applied randomly and as a function only of time. In the space, noises were considered constant assuming that the measurements would be acquired by a thermal infrared camera with a perfect sensitivity.

Many configurations were defined and used as input data for simulations of measured temperatures, so that the estimation can be compared with the defined values, in other words, the exact values.

Two cases were added in this essay with different thermal contact conductance.

Case 1:

$$h_c(t,x) = \begin{cases} 200, & if \quad \begin{cases} 500 \le t \le 1000 & \begin{cases} 0.005 \le x \le 0.01 \\ 0.03 \le x \le 0.035 \end{cases} \\ 2000 \le t \le 2500 & \begin{cases} 0.005 \le x \le 0.01 \\ 0.03 \le x \le 0.035 \end{cases} \end{cases} \\ 1000, & elsewhere \end{cases} \tag{21}$$

Case 2:

$$h_c(t,x) = \begin{cases} \left(10\left(\frac{61}{3000}t - 45\right)^2 + (1025x - 10)^2\right) + 500, & if \quad \left(\left(\frac{61}{3000}t - 45\right)^2 + (1025x - 10)^2\right) < 50 \\ \left(10\left(\frac{61}{3000}t - 15\right)^2 + (1025x - 30)^2\right) + 500, & if \quad \left(\left(\frac{61}{3000}t - 15\right)^2 + (1025x - 30)^2\right) < 40 \\ 1000 & elsewhere \end{cases} \tag{22}$$

Figure 3a shows the thermal contact conductance expressed by Eq. (21) and Fig. 3b shows the estimated thermal contact conductance with noise in the temperature measurements, considering a standard deviation equal to 1°C. In this case, a sudden change in TCC was adopted in four different points.

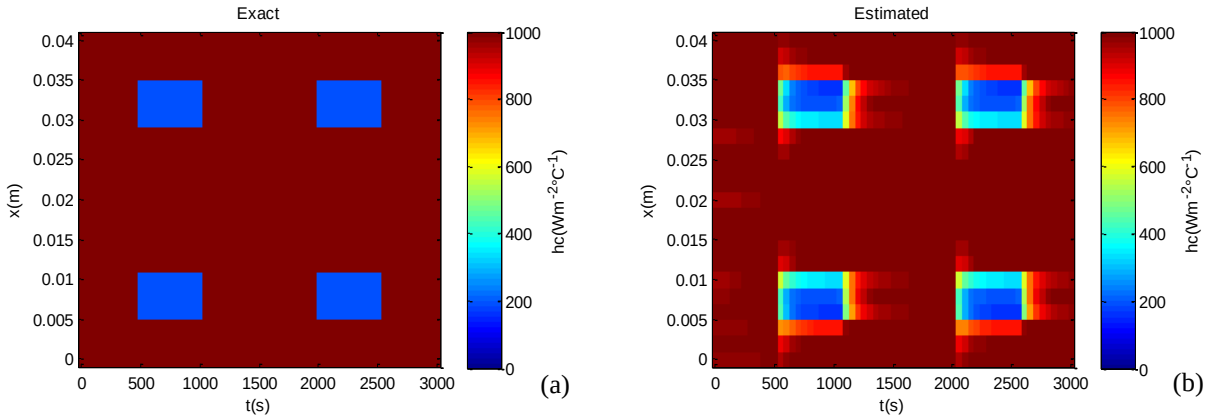


Figure 3. Case 1 - measurement with σ = 1°C of noise: (a) Exact; (b) Estimated

In case 1 with standard deviation equal to 1ºC, the results shown that the change in the thermal conductance can be easily identified both in relation to time and space, although some distinction can be seen in the approximate solution.

Figure 4 show the estimated thermal contact conductance of case 2 which has a softer change on TCC than case 1, the exact plot was obtained according to Eq. (22), the noise applied in this scenario was considering a standard deviation equal to 1°C.

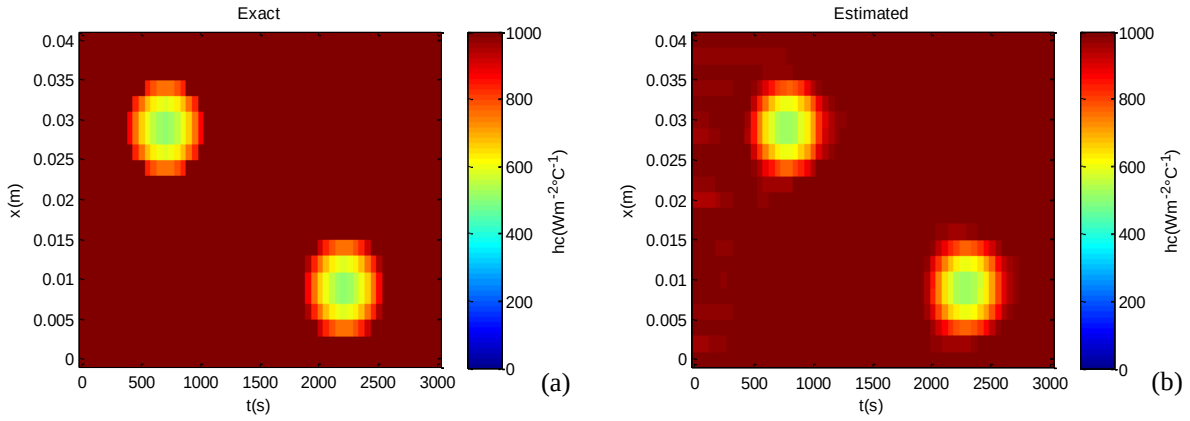


Figure 4. Case 2 - measurement with σ = 1°C of noise: (a) Exact; (b) Estimated

The estimated solution in case 2 obtained a higher accuracy than case 1. In Fig. 4, the difference seen between the exact solution and the approximate solution is small. The main difference in the cases that may justify the greater efficiency in the estimation of case 2 is the smoothness in which the change of TCC occurs in case 2.

Figure 5 shows results considering only 21 temperature measurements for each time.

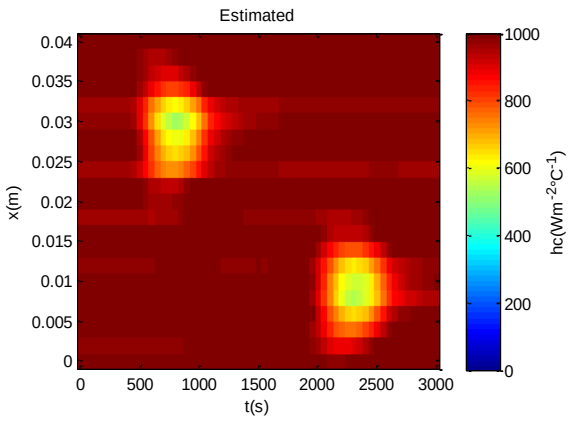


Figure 5. Case 2 - 21 spots measured with σ = 1°C of noise

Reducing the number of temperature measurements, the results presented lower accuracy, but it is still possible to identify the TCC changes.

Figure 6 shows an estimation considering noise with 4°C of standard deviation for the case 1.

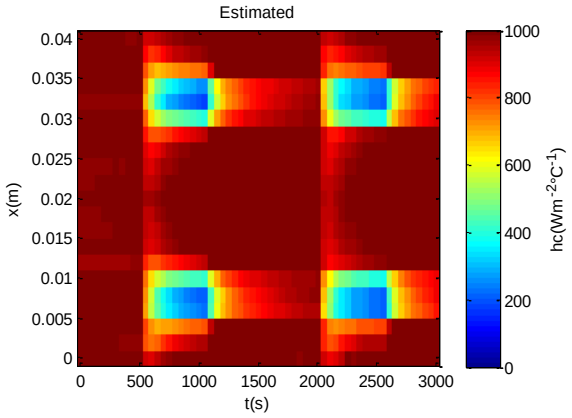


Figure 6. Case 1 - measurement with σ = 4°C of noise

Applying a noise with standard deviation equal 4ºC may be an extreme error, because the current technology allows reducing this uncertainty. But, this situation was done to verify the robustness of the methods studied. Despite of the assigned noise, a reasonable idea of the thermal conductance value is noted.

Table 1 contains Root Mean Square Error (RMSE) for each case with three intensities of noises.

Table 1 – Root Mean Square Error of the estimated thermal contact conductance $h_c(Wm^{-2}°C^{-1})$

| | Measurement at every spots | | 21 spots measured | |
|---|---|---|---|---|
| Noise | Case 1 | Case 2 | Case 1 | Case 2 |
| σ =1°C | 134.39 | 39.75 | 174.95 | 55.34 |
| σ = 2°C | 149.81 | 46.58 | 190.00 | 71.70 |
| σ = 4°C | 170.68 | 57.42 | 205.44 | 77.24 |

As shown in table 1, the RMSE increase according to noise intensity for all scenarios. The estimation found for case 2 presented higher accuracy than case 1 and the results using all temperatures measurements were slightly better than with 21 measurements for each time.

The table 2 represents the computational effort for each test performed.

Table 2 – Total computer effort *time(s)*

| | Measurement at every spots | | 21 spots measured | |
|---|---|---|---|---|
| Noise | Case 1 | Case 2 | Case 1 | Case 2 |
| σ =1°C | 1487 | 1381 | 1393 | 1395 |
| σ = 2°C | 1428 | 1434 | 1434 | 1426 |
| σ = 4°C | 1448 | 1450 | 1464 | 1464 |

In the cases mentioned above, a good approximation of the thermal contact conductance was found requiring almost the same computational efforts for different situations analyzed. Applying high noises as function of time and obtaining good results led to understand that the methodology for this study was robust.

## 4. CONCLUSIONS

This study shows the possibility to apply the Unscented Kalman Filter to determine failure on the contact interface in a laminated composite through the estimation of the thermal contact conductance. The direct problem which is composed by a heat conduction problem was solved by method of lines and temperature measurements used in the estimation were obtained through simulations representing a thermal infrared camera.

The results showed that thermal contact conductance can be estimated using Unscented Kalman Filter. The cases analyzed have shown effectiveness by indicating promising and accurate results. In case 1, the thermal contact conductance change suddenly from $1000Wm^{-2}°C^{-1}$ to $200Wm^{-2}°C^{-1}$ and the estimation showed that the error was higher

than case 2, in which the thermal contact conductance change was smoothly with minimum value equal to $500 Wm^{-2}°C^{-1}$.

The estimation using every temperature measurements was better than the estimation considering only 21 temperature measurements and the computational effort was not reduced when using fewer measurements. Then, for the cases performed, it is better to use the maximum number of measured temperatures allowable.

In this study, the noises applied were only a function of time, so future works will add noise as a function of space representing the sensitivity of an infrared camera.

## 5. ACKNOWLEDGEMENTS

This work was supported by CAPES and FAP/UFES. The authors would like to thank the University of Vila Velha for making the laboratories available for this study.

## 6. REFERENCES

Abreu, L. A., Orlande, H. R. B., Kaipio, J., Kolehmainen, V., Cotta, R. M. and Quaresma, J. N. N., 2014. "Identification of contact failures in multilayered composites with the markov chain monte carlo method". *Journal of Heat Transfer*, Vol. 136, p. 1-9.

Burghold, E., Frekers, Y. and Kneer, R., 2015. "Determination of time-dependent thermal contact conductance through IR-thermography". *International Journal of Thermal Sciences*, Vol. 98, p. 148-155.

Colaço, M. J. and Alves, C. J. S., 2015. "A backward reciprocity function approach to the estimation of spatial and transient thermal contact conductance in double-layered materials using non-intrusive measurements". *International Journal of Computation and Methodology*, Vol. 68, p. 117-132.

da Silva, W. B., Dutra, J. C. S., Abreu, L. A. S., Knupp, D. C., Silva Neto, A. J., 2016. "Estimation of timewise varying boundary heat flux via bayesian filters and markov chain monte carlo method". *Conveción científica de ingniería y arquitectura*.

Gay, D., Hoa, S. V. and Tsai, S. W., 2003. *Composite Materials Design and Application*. CRC Press, Boca Raton, 4th edition.

Julier, S. J. and Uhlmann, J. K., 1997. "A New Extension of the Kalman Filter to Nonlinear Systems". *Proc. SPIE*, Vol. 3068, p. 182-193.

Lee, S. and Knauss, W. G., 2000. "Failure of laminated composites at thickness discontinuities under complex loading and elevated temperatures". *International Journal of Solids and Structures*, Vol. 37, p. 3479-3501.

Rezende, M. C. and Botelho, E. C., 2000. "O uso de compósitos estruturais na indústria aeroespacial". *Ciência e Tecnologia*, Vol. 10, p. 4-10.

Sadiku, M. N. O. and Obiozor, C. N. A., 2000. "A simple introduction to the method of lines". *International Journal of Electrical Engineering Education*, Vol. 37, p. 282-296.

Ventura, A. M. F. M., E. C., 2009. "Os compósitos e a sua aplicação na reabilitação de estruturas metálicas". *Ciência & Tecnologia dos Materiais*, Vol. 21, p. 10-19.

Wan, E. A. and van der Merwe, R., 2000. "The unscented Kalman filter for nonlinear estimation". *IEEE*, p. 153-158.

## 7. RESPONSIBILITY NOTICE

The authors are the only responsible for the printed material included in this paper.